行政院國家科學委員會專題研究計畫 成果報告

石門水庫集水區崩塌災害地理資訊模型之建立—應用可信度因子分析及羅吉斯迴歸模型的比較研究
研究成果報告(精簡版)

計 畫 類 別 ：個別型
計 畫 編 號 ：NSC 95-2415-H-002-031-
執 行 期 間 ：95 年 08 月 01 日至 96 年 10 月 31 日
執 行 單 位 ：國立臺灣大學地理環境資源學系暨研究所

計 畫 主 持 人：張康聰
共 同 主 持 人：林俊全
計畫參與人員：碩士班研究生-兼任助理：顏士閔、姜壽浩

報 告 附 件 ：國際合作計畫研究心得報告

處 理 方 式 ：本計畫可公開查詢

中 華 民 國 96 年 10 月 19 日

1. Introduction

It is well known that many landslides are triggered by rainfall. How to incorporate rainfall into landslide modelling and prediction is therefore an important research topic. The literature has so far suggested three general approaches for relating rainfall to landslide research. First, researchers have attempted to find landslide-triggering rainfall thresholds (Wieczorek and Glade 2005; Guzzetti *et al.* 2007). Campbell (1975) reported rainfall intensity and antecedent rainfall thresholds that could trigger soil slips in the Santa Monica Mountains of southern California. Caine (1980) produced a limiting curve for shallow landslides by using rainfall intensity and duration from 73 observations worldwide. These two early works were followed by numerous studies relating initiation of landslides to minimum rainfall thresholds (Cannon and Ellen 1985; Au 1993; Larsen and Simon 1993; Finlay *et al.* 1997; Guzzetti *et al.* 2004; Baum *et al.* 2005; Chen *et al.* 2005; Cannon *et al.* 2007; Chen *et al.* 2007; Floris and Bozzano 2007), antecedent rainfall conditions (Crozier 1999; Glade *et al.* 2000; Ibsen and Casagli 2004; Cardinali *et al.* 2006), and both antecedent rainfall and rainfall conditions (Aleotti 2004; Godt *et al.* 2006).

Second, rainfall has been used as an input to process-based landslide models. As pore water pressure above a hydrologic impeding layer increases due to rain water, the pore water pressure can be included in the infinite slope equation to estimate slope

stability (Montgomery and Dietrich 1994; Wu and Sidle 1995; Pack *et al.* 1999; Casadei *et al.* 2003; Meisina and Scarabelli 2007). Variations to this general approach have also been developed. For example, pore water pressure response to transient unsaturated flow can be incorporated into a model to see the effect of rainfall intensity and duration (Iverson 2000; Morrissey *et al.* 2004; Baum *et al.* 2005).

Third, at least one study has used rainfall as a dynamic explanatory variable along with the static variables of geologic and geomorphic factors in logistic regression for landslide modelling (Dai and Lee 2003). Other studies have not done so for different reasons. Ohlmacher and Davis (2003) claimed that it was impossible to consider combinations of rainfall intensity, rainfall duration, and antecedent moisture conditions for landslide modelling. Ayalew and Yamagishi (2005) assumed uniform precipitation over their study area (central Japan).

Regardless of the approach, the scarcity of rain gauges has been a common problem of using rainfall for landslide modelling and prediction, especially in mountainous areas. For example, Guzzetti *et al.* (2004) had seven rain gauges available for a study area of 5418 km^2. Researchers have handled insufficient local data by using reference gauges (e.g., Aleotti 2004), Thiessen polygons (e.g., Godt *et al.* 2006), or spatial interpolation (e.g., Guzzetti *et al.* 2004). Nevertheless, results have been unsatisfactory (Casadei *et al.* 2003).

Radar data can provide an alternative to rain gauges. The use of radar data for landslide studies is not new. Campbell (1975) overlaid air traffic control radar maps with soil-slip locations. More recently, rainfall data derived from NEXRAD (NEXt generation RADar) reflectivity imagery have been used for predicting debris flows (Morrissey *et al.* 2004; Chen *et al.* 2007). Compared to the sparse distribution of rain gauges, the high spatial and temporal resolutions of the NEXRAD imagery are highly desirable for landslide studies at the local or watershed level. However, to apply NEXRAD imagery effectively in landslide studies requires selecting a rigorous method for estimating rainfall data from the imagery and finding a reliable statistical model for linking rainfall and landslide.

This paper presents a new and innovative approach to incorporate radar-derived rainfall data into landslide modelling. Using a method developed by Taiwan's Central Weather Bureau (CWB), the study first estimated rainfall data from radar measurements associated with a typhoon (tropical cyclone). Then it derived a landslide prediction model by having maximum rainfall intensity and total duration as the explanatory variables. The model was later validated with estimated rainfall data associated with another typhoon. Satisfactory results from model validation suggest that the model is capable of predicting landslide occurrence by using critical rainfall data from a typhoon event. The model can help develop a real-time landslide

monitoring system during a typhoon and, potentially, a warning system for landslides associated with an approaching typhoon.

2. Study Area and Data

2.1. Study Area

The 760 km^2 study area is located in the Shihmen Reservoir watershed in northern Taiwan (Figure 1). Elevations in the watershed range from 135 m in the northwest to 3529 m in the southeast, with generally rugged topography. Nearly 90% of the study area is forested. The climate is influenced by typhoons in summer and the northeast monsoon in winter. The mean annual temperature is 21 ^oC, with a mean monthly temperature of 27.5 ^oC in July and 14.2 ^oC in January. The annual precipitation averages 2370 mm. Because of the aforementioned typhoons, large rainfall events usually happen from May to September.

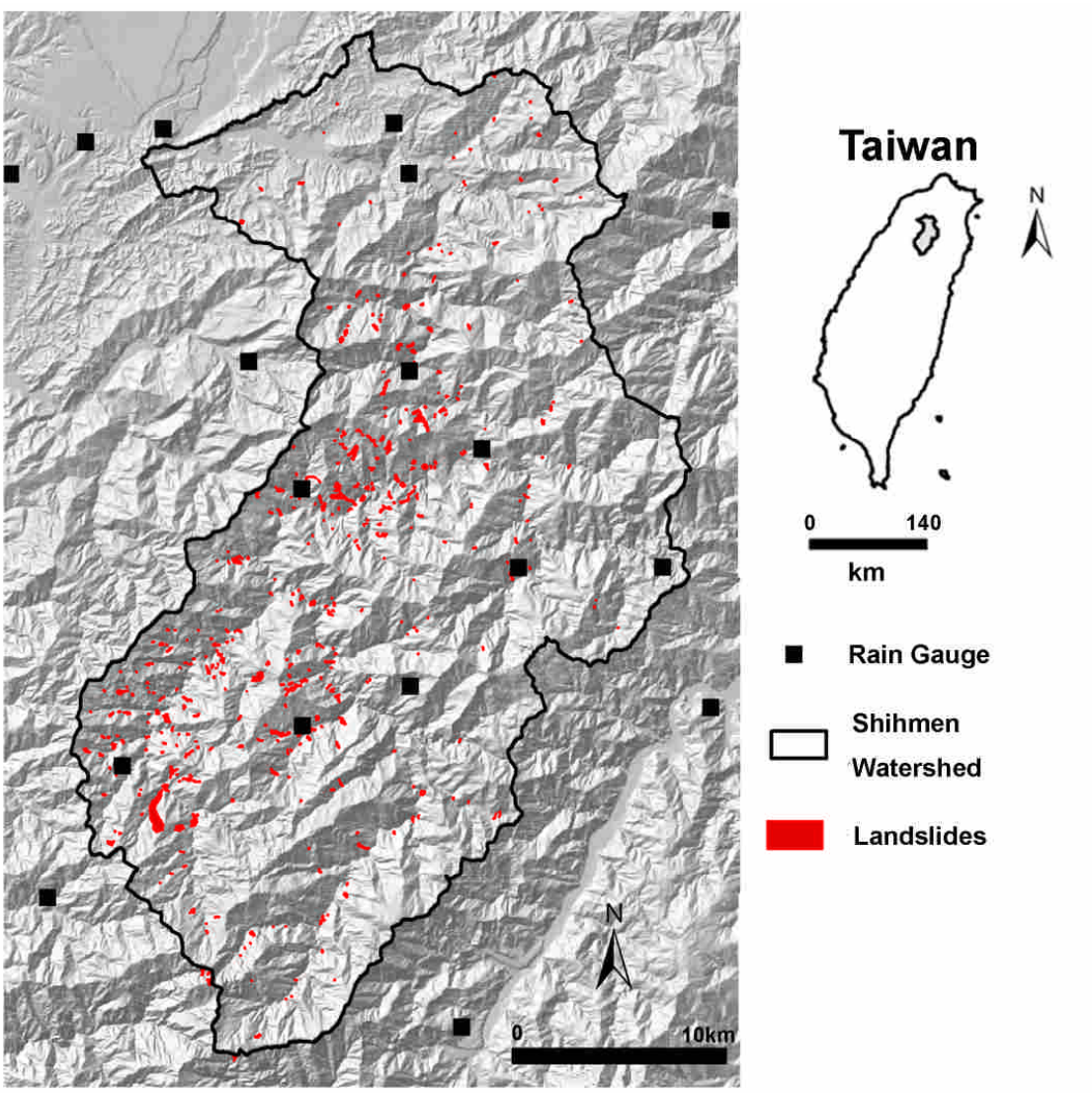

Figure 1. Study area and landslides triggered by Typhoon Aere.

2.2. Typhoon Aere

Taiwan is an island, about 380 km long and 140 km wide, separated by the Strait of Formosa from southeastern China. The island is prone to an average of four to five typhoons originating from the Pacific each year. These intense storms bring torrential rains that trigger landslides in the Central Mountain Range (CMR), which occupies almost two thirds of the island in a north-south orientation. From August 23 to 25, 2004, Typhoon Aere crossed the northern tip of the island in an east-west direction

before turning southwestward. The typhoon affected Taiwan, especially the northern half, for three days. During its peak intensity on August 24, Typhoon Aere had a 200-km storm radius and a low pressure reading of 955 mb, packing winds of 140 km hr^{-1} and gusts to 175 km hr^{-1}. Thirty-four people were killed as a result of the storm, including 15 died as a landslide buried a remote mountain village in the north. The passage of Typhoon Aere brought 1604 mm of rainfall to the study area, with a maximum 24-hr intensity of 51.7 mm hr^{-1} (CWB 2004). The silt accumulation from the upland landslides and stream scouring forced to stop the outlet of drinking water from the Shihmen Reservoir and jammed the water supply pipes for days (Chen *et al.* 2006). Based on the damage to properties and human lives, Typhoon Aere was the worst typhoon that struck northern Taiwan in recent years.

2.3. Landslide Data

Landslides triggered by Typhoon Aere were interpreted and delineated by comparing ortho-rectified aerial photographs taken before and after the typhoon. These colour orthophotographs were compiled by the Aerial Survey Office of Taiwan's Forestry Bureau from the stereo pairs of 1:5000 aerial photographs. They have a pixel size of 0.35 m and an estimated horizontal accuracy of 0.5 m. For model validation, this study interpreted and delineated landslides triggered by Typhoon Haitang (July 17 to 20, 2005) from 2-m FORMOSAT-2 panchromatic satellite images. Table 1 shows the

dates of flights of aerial photographs and satellite images.

Table 1. Image data sources

Events	Aerial Photograph Sets	Satellite Image Sets*
Typhoon Aere	2004/08/06	--
(August 23-25, 2004)	2004/09/02	2004/07/08
Typhoon Haitang	2005/01/17	2005/07/06
(July 17-20, 2005)	--	2005/07/25

-- No Images; *2-m FORMOSAT-2 panchromatic images.

Typhoon Aere triggered 703 landslides of which 50 were enlarged or reactivated old landslides. Typhoon Haitang triggered 1042 landslides of which 455 occurred on existing landslides. Most observed slope failures were shallow landslides on soil mantled slopes with depths less than 2 m. To develop our model, we only considered new landslides triggered by typhoons: 653 by Aere, covering 4.87% of the study area; and 587 by Haitang, covering 2.18% of the study area. Figure 1 shows the spatial distribution of landslides triggered by Typhoon Aere, and Table 2 summarizes the descriptive statistics of landslides triggered by typhoons Aere and Haitang.

Table 2. Descriptive statistics of landslide areas (ha) triggered by typhoons

Typhoon	Number	Area	Maximum	Minimum	Mean	St. Dev.
Aere	653	369.7	46.7	<0.01	0.57	2.1
Haitang	587	94.9	3.0	<0.01	0.16	0.2

2.4. Rainfall Radar Data

Taiwan has over 400 rain gauge stations of which most are located in the lowland areas on the west side of the mountain range. To better understand the spatial distribution of precipitation in mountainous areas, the CWB has collaborated with the U.S. National Oceanic and Atmospheric Agency's National Severe Storms Laboratory to deploy the QPESUMS system (quantitative precipitation estimation and segregation using multiple sensors) (Vieux *et al.* 2003). The system uses four Doppler weather radar (WSR-88D) sites to cover the island and the adjacent ocean. It records base reflectivity with a spatial resolution of 0.0125° (~ 1.25 km) in both longitude and latitude and a temporal resolution of 10 minutes.

The CWB provided radar base reflectivity data for August 23 to 25, 2004, corresponding to the event of Typhoon Aere, for the study area. We also secured ground rainfall measurements for the same time period from 19 automatic rain gauges of which 10 are located within the study area (Figure 1). Likewise, we obtained radar

reflectivity data and rainfall measurements associated with Typhoon Haitang for model validation.

3. Analysis

3.1. Rainfall Estimation

Developed by the CWB, the method for estimating ground-level area rainfall from radar measurements involves two basic steps. First, radar reflectivity *Z*, measured in decibels (db), is converted into rainfall rate *R*, measured in mm hr^{-1}, by the following *Z-R* power relationship (Marshall *et al.* 1947; Wilson 1970):

$$Z = 32.5R^{1.65} \quad (1)$$

The parameter values of 32.5 and 1.65 proposed by Xin *et al.* (1997) are reported to be more accurate than other values for fast moving convective storms.

Rainfall estimates can be improved when rain gauge observations are used to calibrate radar data (Brandes 1975). The calibration method developed by the CWB uses the inverse distance weighted method (IDW) to first create a grid representing the deviations between *R* and hourly rainfall measurements. IDW is a spatial interpolation method. The weight for IDW is defined by:

$$dev_0 = \frac{\sum dev_i W_i}{\sum W_i} \quad (2)$$

$W_i = 1 / d_i^2$, if $d_i <= 30$ km; $W_i = 0$, otherwise

where dev_0 represents the estimated deviation at cell 0, dev_i the deviation at rain gauge

i, W_i the weight at rain gauge i, and d_i the distance between cell 0 and rain gauge i. To complete the calibration, the deviation grid is added to the R grid to calculate the final calibrated rainfall grid.

For this study, we summed the 10-minute radar reflectivity data by hour and divided the sum by six for the hourly average. Then we followed equations (1) and (2) to convert the hourly average reflectivity data into hourly rainfall data. This conversion was performed for typhoons Aere and Haitang. The projection of the hourly rainfall grid from geographic to plane coordinates resulted in a 36 by 55 grid with a spatial resolution of 1 km.

Using the hourly rainfall data, we derived various measures of rainfall intensity, total, and duration associated with Typhoon Aere. Figures 2a, 2b, and 2c display the maximum 3-hr rainfall intensity, total rainfall, and total duration, respectively. The spatial distributions of maximum 3-hr rainfall intensity and total rainfall show similar pattern. Both have the highest values in the southwestern and western parts of the watershed, near the ridge that faced the dominant southwesterly and westerly winds during the passage of Typhoon Aere. Table 3 shows the descriptive statistics of these various rainfall factors as well as the correlation coefficients (r) between landslide density (number of landslides km^{-2}) and each factor. Maximum 3-hr intensity and maximum 6-hr intensity have higher r values than other factors, although the

differences are small.

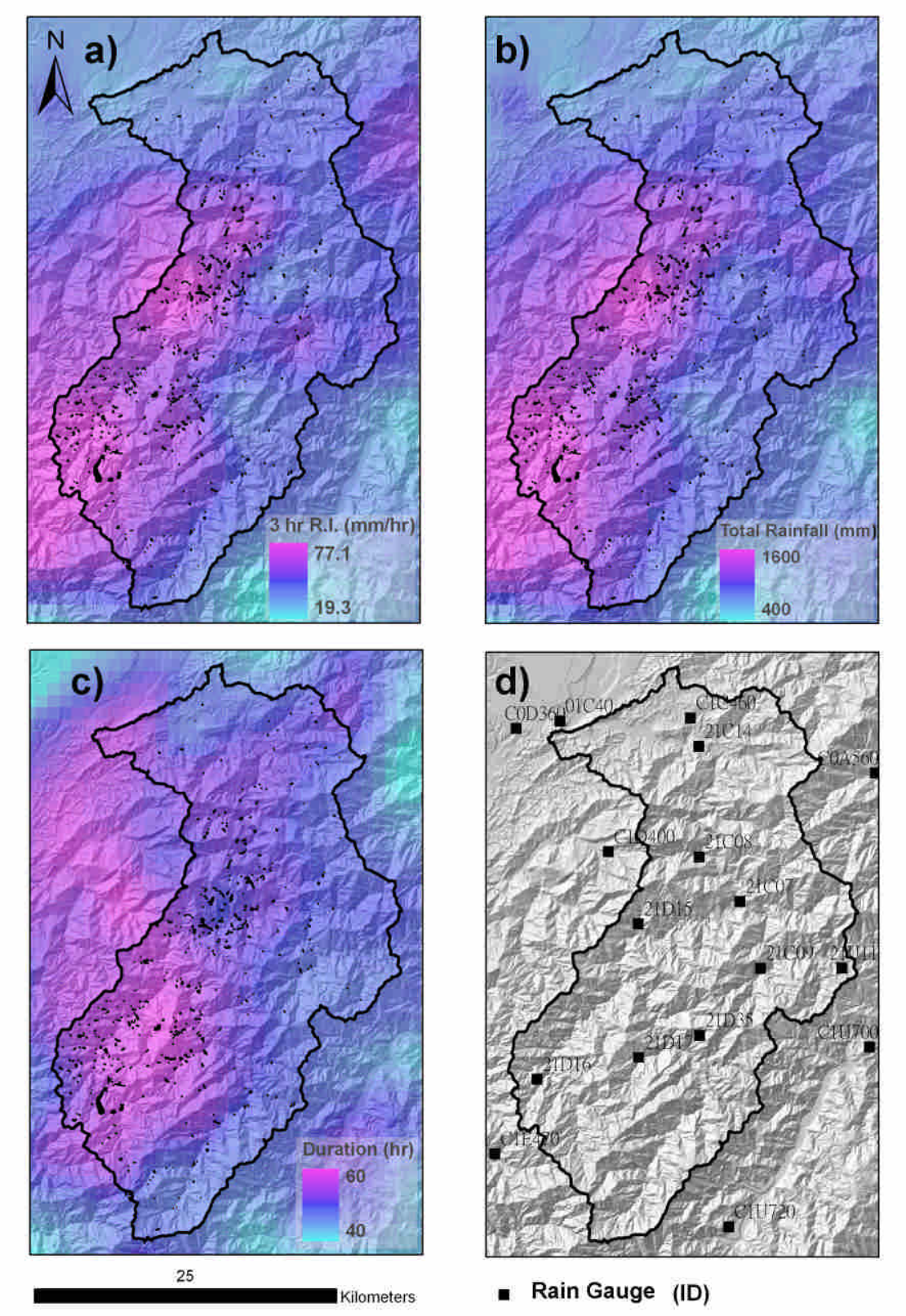

Figure2. Spatial distributions of rain factors (a. 3-hr rain intensity; b. total rainfall; c.

rainfall duration) and rain gauges (d).

Table 3. Rainfall factors and statistics

Factors		Max	Min	Mean	St. Dev.	*r**
	Max 1hr	86.5	38.4	58.7	11.3	0.24**
	Max 3hr	77.1	33.5	53.6	10.4	0.26**
Rainfall Intensity	Max 6hr	75.9	32.6	51.8	10.3	0.25**
(mm/hr)	Max 12hr	64.2	25.3	43.3	9.1	0.24**
	Max 24hr	51.7	19.4	33.6	7.4	0.21**
	Average	28.8	12.5	19.9	3.6	0.21***
Total Rainfall (mm)		1604.0	678.3	1111.5	215.2	0.23**
Total Duration (hr)		58	53	55.7	1.4	0.23***

*Correlation coefficient between rainfall factor and landslide density

** Significant at 1% level

*** Significant at 5% level

3.2 Logistic Regression

Logistic regression is useful when the dependent variable is categorical (e.g., presence or absence) and the explanatory variables are categorical, numeric, or both (Menard 2002). The logit model from a logistic regression has the following form:

$$\text{logit}(y) = a + b_1x_1 + b_2x_2 + b_3x_3 + \ldots + e \quad (3)$$

where the logit of y is the dependent variable, x_i is the explanatory variable i, a is a constant, b_i is the regression coefficient i, and e is the error term. The logit of y is the natural logarithm of the odds:

$$\text{logit}(y) = \ln\left(\frac{p}{1-p}\right) \quad (4)$$

where p is the probability of the occurrence of y and $p/(1 - p)$ is the odds. To convert logit (y) back to the probability p, equation (4) can be rewritten as:

$$p = \frac{\exp(a + b_1x_1 + b_2x_2 + b_3x_3 + ...)}{1 + \exp(a + b_1x_1 + b_2x_2 + b_3x_3 + ...)} \quad (5)$$

A logit model can be evaluated by the receiver operating characteristic (ROC). The ROC measures the fitness of a model on the basis of true positive (proportion of incidences correctly reported as positive) and false positive (proportion of incidences erroneously reported as positive) (Pontius and Batchu, 2003). Typically, a probability value of 0.5 is used to determine whether the model has made a correct prediction (> 0.5) or not (< 0.5). Additionally, Cox and Snell R^2 and Nagelkerke R^2 measure how well the explanatory variables can predict and explain the dependent variable. Cox and Snell R^2 cannot achieve a maximum of 1, whereas Nagelkerke R^2 stretches the R^2 value to range from 0 to 1.

For this study, the dependent variable (y) represented landslide (1) or stable area cell (0) and the explanatory variables were maximum 3-hr rainfall intensity (x_1) and total duration (x_2). Largely dependent on the data source, rainfall variables examined

in previous studies can be generally grouped into two categories. The first category uses rainfall intensity and duration (Caine 1980; Cannon and Ellen 1985; Larsen and Simon 1993; Finlay *et al.* 1997; Aleotti 2004; Godt *et al.* 2006), and the second uses total or cumulative rainfall (Au 1993; Dai and Lee 2003; Guzzetti *et al.* 2004; Ibsen and Casagli 2004). This study followed the first category of studies but chose maximum 3-hr rainfall intensity instead of average intensity because maximum 3-hr rainfall intensity had a slightly higher *r* value with landslide density.

4. Results

4.1. Logit Model

The logit model is significant at the 0.01 level, with ROC = 0.76, Cox & Snell R^2 = 0.27, and Nagelkerke R^2 = 0.36. Both explanatory variables are significant at the 1% level, with total duration being slightly more important than maximum 3-hr intensity in explaining landslide occurrence (Table 4).

Table 4. Logistic regression results[a]

Variables	β	S.E.	Wald	df	*p*	Exp(β)
Total duration (hr)	0.25	0.06	17.90	1	<0.01	1.29
Max 3-hr intensity (mm/hr)	0.10	0.01	119.50	1	<0.01	1.11
Constant	-18.99	2.98	57.12	1	<0.01	0.00

[a] β represent the estimated regression coefficients for the explanatory variables, with

the standard error (S.E.) given. The Wald statistic is the ratio of the β to S.E. of the regression coefficient squared. df is the degree of freedom. The significance of each explanatory is given by the *p* value. Exp(β) is the predicted change in odds for a unit increase in the explanatory variable.

4.2. Critical Rainfall Conditions

To use rainfall data for predicting landslides, critical rainfall intensity and total duration can be derived from the logit model. Substituting logit (*y*) by equation (4) and ignoring the error term, equation (3) becomes:

$$\ln(\frac{p}{1-p}) = a + b_1 x_1 + b_2 x_2 \quad (6)$$

Equation (6) can be rewritten as:

$$x_1 = \frac{1}{b_1}\left[\ln(\frac{p}{1-p}) - (b_2 x_2 + a)\right] \quad (7)$$

By specifying the *p* value (e.g., 0.5) and an x_2 value in equation (7), we can compute a corresponding x_1 value. By going through the computation twice, we can get two pairs of x_1 and x_2 values to plot a straight line representing the specified *p* value (e.g., 0.5). Figure 3 shows such lines representing the probabilities of landslide occurrence at 0.2, 0.4, 0.5, 0.6, and 0.8. Equation (7) is hereafter referred to as the *probability model*. Figure 3 also shows dots for landslide and stable-area cells. The location of a dot or cell corresponds to its maximum 3-hr rainfall intensity and total duration values, and the colour shows whether landslide is present in the cell or not. Figure 4a plots

landslides triggered by Typhoon Aere against calculated probabilities from equation (7). As to be expected, most landslides fall within areas of high probabilities.

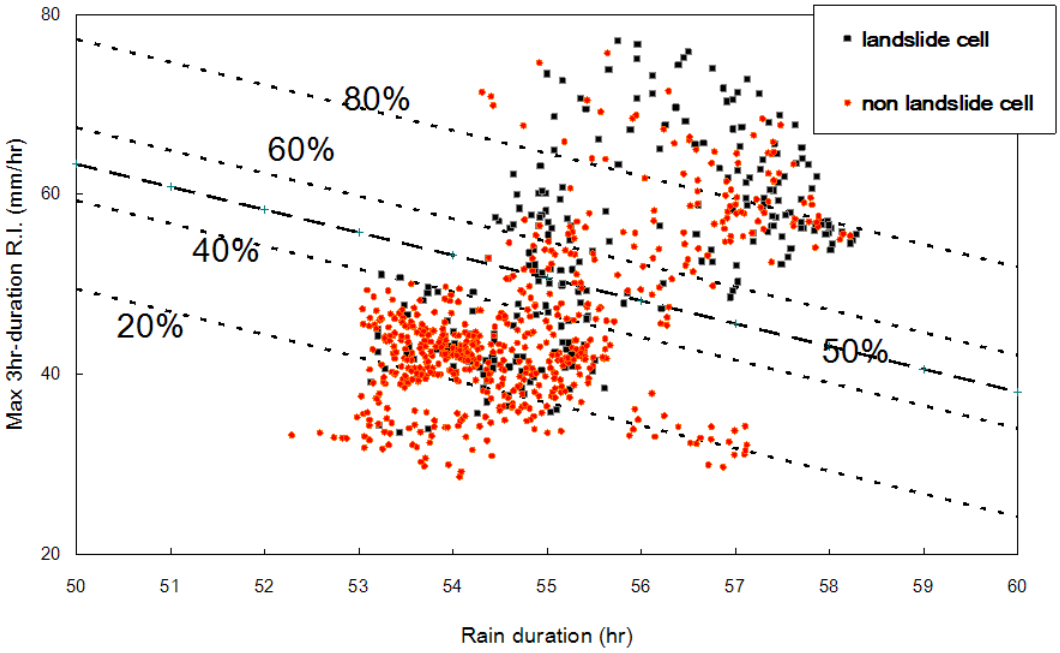

Figure 3. Critical rainfall conditions for triggering landslides. The lines show different probabilities for landslide occurrence derived by using equation (7).

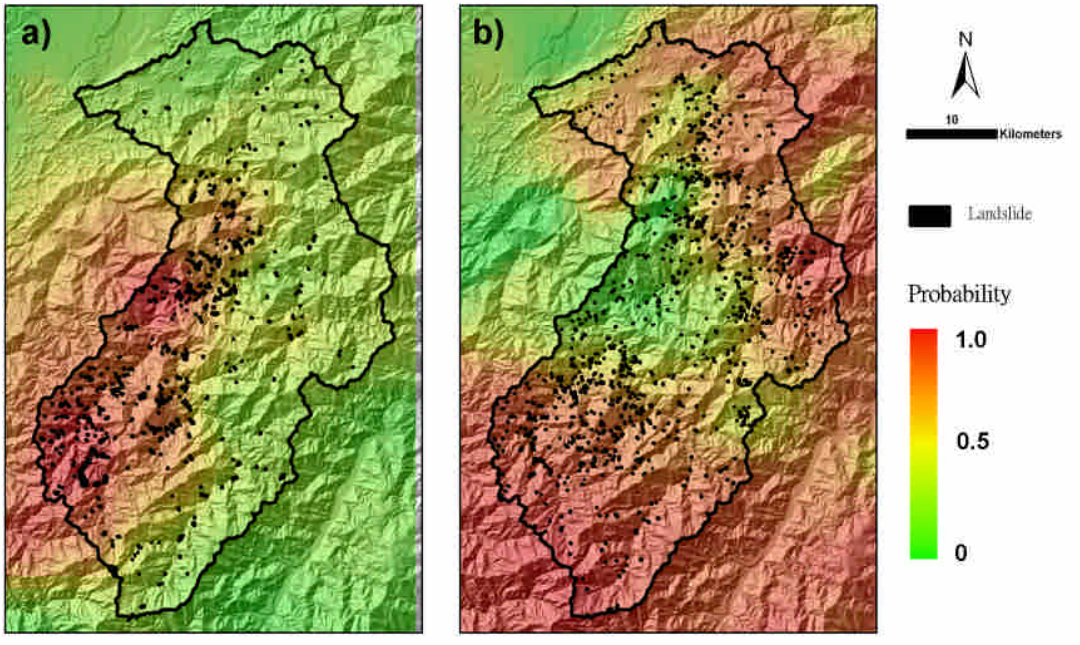

Figure 4. Probability maps of landslide occurrence derived from the model and landslides triggered by Typhoon Aere (a) and Typhoon Haitang (b).

4.3 Model Validation

Landslides triggered by Typhoon Haitang were used for validating the probability model derived from the landslide and rainfall data associated with Typhoon Aere. Using 0.5 as the threshold, the model correctly predicted 81.6% of landslides triggered by Typhoon Haitang. In other words, 81.6% of landslides fall within areas with probabilities greater than 0.5 as predicted by the model (Figure 5). This is visually confirmed in Figure 4b, which plots landslides triggered by Typhoon Haitang against calculated probabilities from equation (7).

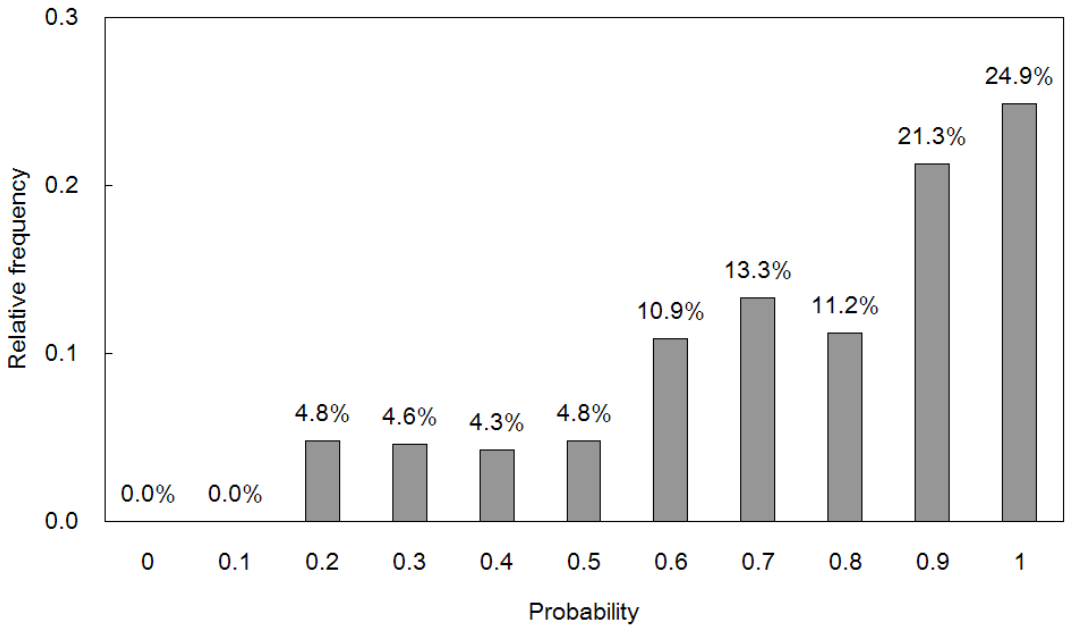

Figure 5. A comparison of relative frequencies of landslides triggered by Typhoon Haitang and probabilities calculated from the model developed from the landslide and

rainfall data associated with Typhoon Aere.

5. Discussion

5.1. The Probability Model vs. Minimum Rainfall Threshold

The probability model that this study has developed differs from minimum rainfall thresholds of previous studies in two fundamental aspects. First, the probability model is a spatially explicit model, which is based on logistic regression that statistically separate landslides from stable areas by maximum 3-hr rainfall intensity and rainfall duration. In contrast, a minimum rainfall threshold represents the lower bound of a log-log plot of rainfall data that have resulted in landslides without considering the locations of landslides and stable areas. Second, the probability model computes a probability for a given combination of rainfall values and offers a measure of the likelihood of landslide occurrence. In comparison, a minimum rainfall threshold simply suggests that, if a rainfall event exceeds the threshold, it will likely trigger landslides. No measure of confidence is provided with such prediction. Given these two differences, we feel that the probability model is better suited for a landslide monitoring or warning system than the minimum rainfall threshold.

5.2. Radar Data for Landslide Studies

The high spatial and temporal resolutions of the NEXRAD reflectivity imagery are desirable for watershed-scale landslide modelling, either process-based or empirically

based. But the *Z-R* relationship for converting radar reflectivity data to rainfall rate can be complicated by ground clutter, beam blockage, close clustering of cells, and differences in precipitation echoes between water droplets and ice particles and between different-sized water droplets (Howard *et al.* 1997; Steiner and Smith 2002; Wilson 2005).

This study adopted a method developed by Taiwan's CWB for estimating rainfall from radar measurements. Because we used all 19 automatic gauge stations in and around the study area for calibration, we could not perform an accuracy assessment of radar-derived rainfall data. However, previous studies have shown the robustness of the CWB method. Based on two typhoon events, Chang *et al.* (2006) reported that calibrated rainfall estimates from QPESUMS reflectivity imagery deviated from ground measures of 100 gauge stations in Taiwan by less than 1 mm for hourly rainfall, 12 to 34 mm for daily rainfall, and 29 to 79 mm for total rainfall. Chen *et al.* (2007) found that calibrated rainfall data by QPESUMS estimation agreed well with those from four ground-based stations in central Taiwan, with the correlation coefficients all above 0.9 between the two. Both studies therefore support the QPESUMS system and the CWB method for rainfall estimation.

Rainfall data derived from QPESUMS imagery have a spatial resolution of 1.25 km (1 km after projection for this study). Although this resolution is higher than that

of ground-based rain gauges, it still cannot match that of landslides delineated and mapping on aerial photographs or high-resolution satellite images. On the other hand, landslide data cannot match the temporal resolution (10 minutes) of QPESUMS imagery. In fact, the timing of landslides is usually gathered from interviews of local residents and its accuracy can only be described as reasonably accurate (e.g., Guzzetti *et al.* 2004). The incompatibility of scales/resolutions is common in landslide studies (e.g., 1:5000-scale soil map vs. 1:100,000-scale geology map), but it can create problems in interpreting and applying results. How to match landslide and rainfall data in both spatial and temporal resolutions is certainly an important topic for future investigation.

5.3 Applications of the Model

The probability model that this study has developed is simple to use: given maximum 3-hr rainfall intensity and total rainfall duration, the model computes probabilities for landslide occurrence on a cell basis. It can be part of a real-time landslide monitoring system in which the two rainfall variables calculated from the QPESUMS system are entered to compute the probability of landslide occurrence at a regular interval (e.g., every six hours) during a typhoon event. The probability map thus derived will show which areas are likely to have landslide occurrence, and the difference in probability can assist an emergency management team in decision making.

The model can also be used as an aid for landslide delineation and mapping following a typhoon event. A mask based on the model or a model with additional variables can highlight areas that are more likely to have landslides, thus facilitating such tasks as coordinating mitigation efforts. For example, if we add elevation, slope, and lithology as explanatory variables to the logit model in this study, the model has ROC = 0.78, Cox & Snell R^2 = 0.32, and Nagelkerke R^2 = 0.42. This model can therefore better assist in locating areas that are more prone to landslides than the initial logit model with only two rainfall variables.

But to use the probability model for a landslide warning system will require a robust typhoon precipitation model at a high spatial resolution. Because Taiwan is extremely vulnerable to the damages from typhoons, numerical models for simulating typhoons have been a top research priority (Wu and Kuo 1999). The fifth-generation Pennsylvania State University-National Centre for Atmospheric Research Mesoscale Model (MM5) has been used in several recent studies to simulate the rainfall distribution associated with a typhoon (Wu *et al.* 2002; Witcraft *et al.* 2005; Yang and Ching 2005). A typhoon rainfall climatology-persistence (R-CLIPER) has also been used for rainfall estimation in the 2004 and 2005 typhoon seasons (Cheung *et al.* 2006). Although these studies all reported good simulation or prediction results, they were designed for the Taiwan area at a spatial resolution of 2.2 km or coarser. The

spatial scale issue must be resolved before the integration of a typhoon model and this study's landslide probability model can be realised for a watershed-level warning system.

6. Conclusion

This study compiled Doppler weather radar reflectivity data during Typhoon Aere (August 2004), estimated rainfall from radar data, and used maximum 3-hr rainfall intensity and rainfall duration as the explanatory variables in logistic regression for a landslide prediction model. The logit model had a ROC of 76%. Results of model validation showed an accuracy rate of 82% in predicting landslides triggered by Typhoon Haitang (July 2005). This cell-based model can be part of a landslide warning system by incorporating predicted rainfall data from a typhoon precipitation model. It can also be part of a real-time landslide monitoring system by being able to compute probabilities of landslide occurrence at a regular interval during a typhoon event. Finally, the model can be used as an analysis mask for landslide delineation and mapping following a typhoon event. Compared to minimum rainfall thresholds of previous studies, this probability model has the distinct advantage of providing a measure of confidence in predicting landslides and landslide locations associated with a typhoon event.

The landslide-rainfall model that this study has developed represents a new

approach to incorporate rainfall into landslide modelling and prediction. Further improvement of the model requires a better integration of landslide data, radar reflectivity data, and estimated typhoon precipitation data in both spatial and temporal resolutions.

References

Aleotti P. 2004. A warning system for rainfall-induced shallow failures. *Engineering Geology* **73**: 247-265.

Au SWC. 1993. Rainfall and slope failure in Hong Kong. *Engineering Geology* **36**: 141-147.

Ayalew L, Yamagishi, H. 2005. The application of GIS-based logistic regression for landslide susceptibility mapping in the Kakuda-Yahiko Mountains, Central Japan. *Geomorphology* **65**: 15-31.

Barm RL, Coe JA, Godt JW, Harp, EL, Reid ME, Savage WZ, Schulz WH, Brien DL, Chleborad AF, McKenna JP, Michael JA. 2005. Regional landslide-hazard assessment for Seattle, Washington, USA. *Landslides* **2**: 266-279.

Brandes EA. 1975. Optimizing rainfall estimates with the aid of radar. *Journal of Applied Meteorology* **14**: 1339-1345.

Caine N. 1980. The rainfall intensity-duration control of shallow landslides and debris flows. *Geografiska Annaler* **62A**: 23-27.

Campbell RH. 1975. *Soil Slips, Debris Flows, and Rainstorms in the Santa Monica Mountains and Vicinity, Southern California*. USGS Professional Paper 851. US Geological Survey: Reston, VA.

Cannon SH, Ellen S. 1985. Rainfall conditions for abundant debris avalanches in the

San Francisco Bay region, California. California *Geology* **38**: 267-272.

Cannon SH, Gartner JE, Wilson RC, Bowers JC, Laber JL. 2007. Storm rainfall conditions for floods and debris flows from recently burned areas in southwestern Colourado and southern California. *Geomorphology*, in press. DOI: 10.1016/j.geomorph.2007.03.019.

Cardinali M, Galli M, Guzzetti F, Ardizzone F, Reichenbach P, Bartoccini P. 2006. Rainfall induced landslides in December 2004 in Southwestern Umbria, Central Italy. *Natural Hazards and Earth System Sciences* **6**: 237-260.

Casadei M, Dietrich WE, Miller NL. 2003. Testing a model for predicting the timing and location of shallow landslide initiation in soil-mantled landscapes. *Earth Surface Processes and Landforms* **28**: 925-950.

Chang C, Sun C, Lay J. 2006. Integration of radar detection and real time rainfall data for estimation during typhoon period. *Environment and Worlds* **13**: 1-22. (in Chinese)

Chen C, Chen T, Yu F, Yu W, Tseng C. 2005. Rainfall duration and debris-flow initiated studies for real-time monitoring. *Environmental Geology* **47**: 715-724.

Chen C, Lee W, Yu F. 2006. Debris flow hazards and emergency response in Taiwan. In *Monitoring, Simulation, Prevention and Remediation of Dense and Debris Flows*, Lorenzini G., Brebbia CA, Emmanouloudis DE. (eds). WIT Press: Southampton, Boston; 311-320.

Chen C, Lin L, Yu F, Lee C, Tseng C, Wang A, Cheung K. 2007. Improving debris flow monitoring in Taiwan by using high-resolution rainfall products from QPESUMS. *Natural Hazards* **40**: 447-461.

Cheung KKW, Huang L, Lee C. 2006. A tropical cyclone rainfall climatology-persistence model for the Taiwan area. *Proceedings: 27th Symposium on Hurricane and Tropical Meteorology*, April 24-28, Monterey, CA.

Crozier MJ. 1999. Prediction of rainfall-triggered landslides: A test of the antecedent water status model. *Earth Surface Processes and Landforms* **24**: 825-833.

CWB (Central Weather Bureau). 2004. http://photino.cwb.gov.tw/tyweb/tyfnweb/htm/2004aere.htm (accessed April 22, 2006).

Dai FC, Lee CF. 2003. A spatiotemporal probabilistic modelling of storm-induced shallow landsliding using aerial photographs and logistic regression. *Earth Surface Processes and Landform* **28**: 527-545.

Finlay PJ, Fell R, Maguire PK. 1997. The relationship between the probability of landslide occurrence and rainfall. *Canadian Geotechnical Journal* **34**: 811-824.

Floris M, Bozzano F. 2007. Evaluation of landslide reactivation: a modified rainfall threshold model based on historical records of rainfall and landslides. *Geomorphology*, in press. DOI: 10.1016/j.geomorph.2007.04.009.

Glade T, Crozier MJ, Smith P. 2000. Applying probability determination to refine landslide-triggering rainfall thresholds using an empirical "Antecedent Daily Rainfall Model". *Pure and Applied Geophysics* **157**: 1059-1079.

Godt JW, Baum RL, Chleborad AF. 2006. Rainfall characteristics for shallow landsliding in Seattle, Washington, USA. *Earth Surface Processes and Landforms* **31**: 97-110.

Guzzetti F, Cardinali M, Reichenbach P, Cipolla F, Sebastiani C, Galli M, Salvati P. 2004. Landslides triggered by the 23 November 2000 rainfall event in the Imperia Province, Western Liguria, Italy. *Engineering Geology* **73**: 229-245.

Guzzetti F, Peruccacci S, Rossi M, Start CP. 2007. Rainfall thresholds for the initiation of landslides. *Meteorology and Atmospheric Physics*, in press. DOI: 10.1007/s00703-007-0262-7.

Howard KW, Gourley JJ, Maddox RA. 1997. Uncertainties in WSR-88D measurements and their impacts on monitoring life cycles. *Weather and Forecasting* **12**: 166-174.

Ibsen M-L, Casagli N. 2004. Rainfall patterns and related landslide incidence in the Porretta-Vergato region, Italy. *Landslides* **1**: 143-150.

Iverson RM. 2000. Landslide triggering by rain infiltration. *Water Resources Research* **36**: 1897-1910.

Marshall JS, Langille RC, Palmer WM. 1947. Measurement of rainfall by radar. *Journal of Meteorology* **4**: 186-191.

Meisina C, Scarabelli S.2007. A comparative analysis of terrain stability models for predicting shallow landslides in colluvial soils. *Geomorphology* **87**: 207-223.

Menard S. 2002. *Applied Logistic Regression Analysis*, 2d ed. Thousand Oaks, CA: Sage.

Montgomery DR, Dietrich WE. 1994. A physically based model for topographic control on shallow landsliding. *Water Resources Research* **30**: 1153-1171.

Morrissey MM, Wieczorek GF, Morgan BA. 2004. Transient hazard model using radar data for predicting debris flows in Madison County, Virginia. *Environmental & Engineering Geoscience* **10**: 285-296.

Ohlmacher GC, Davis JC. 2003. Using multiple logistic regression and GIS technology to predict landslide hazard in northeast Kansas, USA. *Engineering Geology* **69**: 331-343.

Pack RT, Tarboten DG, Goodwin CN. 1999. GIS-based landslide susceptibility mapping with SINMAP, *Proceedings: 34th Symposium on Engineering Geology and Geotechnical Engineering*, April 28-30, Logan, Utah; 219-231.

Pontius RG, Jr., Batchu K. 2003. Using the relative operating characteristic to quantify certainty in prediction of location of land cover change in India. *Transactions in GIS* **7**:

467-484.

Steiner M, Smith JA. 2002. Use of three-dimensional reflectivity structure for automated detection and removal of nonprecipitating echoes in radar data. *Journal of Atmospheric and Oceanic Technology* **19**: 673-686.

Vieux BE, Vieux JE. 2003. Operational deployment of a physics-based distributed rainfall-runoff model for flood forecasting in Taiwan. Paper presented at the International Symposium on Information from Weather Radar and Distributed Hydrological Modelling, July 7-8, 2003, Sapporo, Japan.

Wieczorek GF, Glade T. 2005. Climatic factors influencing occurrence of debris flows. In *Debris Flows Hazards and Related Phenomena*, Jakob M, Hungr O. (eds). Springer: Berlin; 325-362.

Wilson JW. 1970. Integration of radar and raingage data for improved rainfall measurement. *Journal of Applied Meteorology* **9**: 489-497.

Wilson RC. 2005. The rise and fall of a debris-flow warning system for the San Francisco Bay region, California. In *Landslide Hazard and Risk*, Glade T, Anderson M, Crozier MJ (eds). Wiley: Chichester, England; 493-516.

Witcraft N, Lin Y, Kuo Y. 2005. Dynamics of orographic rain associated with the passage of a tropical cyclone over a mesoscale mountain. *Terrestrial, Atmospheric and Oceanic Sciences* **16**: 1133-1161.

Wu C, Kuo Y. 1999. Typhoons affecting Taiwan: current understanding and future challenges. *Bulletin of the American Meteorological Society* **80**: 67-80.

Wu C, Yen T, Kuo Y, Wang W. 2002. Rainfall simulation associated with Typhoon Herb (1996) near Taiwan, Part I: The topographic effect. *Weather and Forecasting* **17**: 1001-1015.

Wu W, Sidle RC. 1995. A distributed slope stability model for steep forested basins. *Water Resources Research* **31**: 2098-2110.

Xin L, Reuter G, Larochelle B. 1997. Reflectivity-rain rate relationships for convective rainshowers in Edmonton. *Atmosphere-Ocean* **35**: 513-521.

Yang M, Ching L. 2005. A modelling study of typhoon Toraji (2001): physical parameterization sensitivity and topographic effect. *Terrestrial, Atmospheric and Oceanic Sciences* **16**: 177-213.

In July 2007 I went to Wageningen University, the Netherlands, to meet with Profs. Tom Veldkamp and Gerald Schoorl. Profs. Veldkamp and Schoorl are developers of the LAPSUS (**L**andsc**A**pe **P**roces**S** modelling at m**U**lti-dimensions and scale**S**), a multi-module dynamic landscape evolution model. Since the trip, we have been working on a joint research project involving graduate students at National Taiwan University and Wageningen University.

In September 2007 I was invited by KITAC Corp in Niigata, Japan to give a keynote speech on my research work on rainfall-triggered landslides. Following the trip, I have been working with Dr. Cheibany of KITAC Corp to test the critical rainfall model that we have developed at National Taiwan University using precipitation and landslide data from Niigata, Japan.